EurJIC
European Journal of Inorganic Chemistry

Research Article
doi.org/10.1002/ejic.202300276

Chemistry Europe
European Chemical Societies Publishing

www.eurjic.org

Hexacoordinated M^{IV} (M=Ti, Zr, Hf) Tetrachlorido Complexes with Chelating Dithienylethane Based 1,2 Diketone Ligand – π-Conjugation as Decisive Factor for Axial Chirality Mode

Dirk Schlüter,[a] Daniel Duvinage,[a] Robert Langer,[b] and Matthias Vogt*[a, b]

1,2-bis(2,5-dimethylthiophen-3-yl)ethane-1,2-dione (**1**, *DTEthane*) reacts with MCl_4 metal precursors of group four (M=Ti, Zr, Hf) via coordination of the carbonyl groups. The molecular structure of complex **2–4** were determined in scXRD studies in the solid state and characterized by means of multi-nuclear and multi-dimensional NMR spectroscopy in solution. While the resulting titanium complex [$TiCl_4$(*DTEthane*)] **2** shows a monomeric structure, where **1** binds in a bidentate fashion, complexes with a Zr (**3**) and Hf (**4**) center have dimeric scaffolds in which the ligands adopt a bridging mode. Quantum chemical calculations using density functional theory (G16, B97D3/def2-TZVP) were used to evaluate the general trend of dimer formation (Ti < Zr < Hf). The molecular structures derived from both scXRD and the DFT optimized structures reveal the carbonyl groups in conjugation with the adjacent thiophene substituent. As a result, they are coplanar and rotation about the two C–C axes (C1–C7; C8–C9) is restricted allowing for only one chiral axis along C7–C8. This gains special importance with respect to previously described complexes carrying the closely related 1,2-endiolato ligand (1,2-bis(2,5-dimethylthiophen-3-yl)ethene-1,2-diolate), in which no coplanarity of the thiophene rings to their neighboring metallacycle was observed allowing for two chiral axes. Noteworthy, further DFT calculations addressing the pathway of racemization found transition states, which are characterized by contrary rotations of both thiophene rings and a loss of conjugation rather than a direct rotation around the axis C7–C8.

Introduction

Ever since their first synthesis by Irie and Mohri in the late 1980s, dithienylethenes (DTE) have gained significant attention as photochemically reversible photochromic compounds.[1] Bearing a hexatriene-motif, they are able to undergo a light-induced switching between the ring-open and the ring-closed isomer (Scheme 1 **A**), which often is accompanied by a significant color change. They can therefore be considered to feature an 'on'- and 'off'-state (ring-closed *vs.* ring open-isomer) in analogy to '0' and '1' of the binary system.[2,3] Due to their excellent photochromic properties[1] they are often regarded to hold potential for applications, such as high density optical memory devices,[1,4] logic gates,[5,6] multi responsive molecular switches,[3,7,8] photochromic conducting polymers,[9] selective fluorescent probes for detection of metal ions,[10] photo-responsive self-assemblies at liquid/solid interfaces,[11] photo-responsive building blocks being able to regulate supramolecular architectures,[12,13] photochromic molecular capsules,[14] light-driven actuators,[15,16] and photo-modulating catalysis.[17]

The typical alkene motif, as part of a (metalla) cyclic system[18–20] with the two thiophene groups in mutual *cis*-arrangement, gives rise to two C–C rotational axes and therefore different rotameric configurations can occur. The rotamers can be described according to the alignment of the thiophenes and the observed helicity: That is, two helical structures with antiparallel alignment of the thiophene units in M- and P-helicity, respectively, can arise, as well as a conformer in parallel alignment (see Scheme 1, **A**).[21] As a result, photoirradiation of the helical isomers (P and M) can lead to the ring closed structures encompassing two stereogenic centers with (*R*,*R*) and (*S*,*S*) configuration, respectively. These stereogenic centers are located at the carbon atoms involved in the formation of the new C–C bond.[21,22] Note that only the antiparallel conformers can react via photocyclization.

A particular case of axial chirality with respect to the above mentioned rotamers occurs when they are fully resolvable at ambient temperature meaning that the individual rotamers are 'locked' due to a sufficiently high barrier of interconversion caused by the (sterically) hindered rotation about the two C–C rotational axes.[23] Then, by definition of Ōki,[24] those rotamers

[a] *D. Schlüter, D. Duvinage, Dr. M. Vogt*
Institut für Anorganische Chemie und Kristallographie
Universität Bremen, 28359 Bremen (Germany)
[b] *Prof. Dr. R. Langer, Dr. M. Vogt*
Martin-Luther-Universität Halle Wittenberg
Naturwissenschaftliche Fakultät II
Institut für Chemie – Anorganische Chemie;
Kurt-Mothes-Str. 2, 06120 Halle (Saale) (Germany)
E-mail: matthias.vogt@chemie.uni-halle.de
www.chemie.uni-halle.de

Supporting information for this article is available on the WWW under https://doi.org/10.1002/ejic.202300276

Research Article
doi.org/10.1002/ejic.202300276

Chemistry Europe
European Chemical Societies Publishing

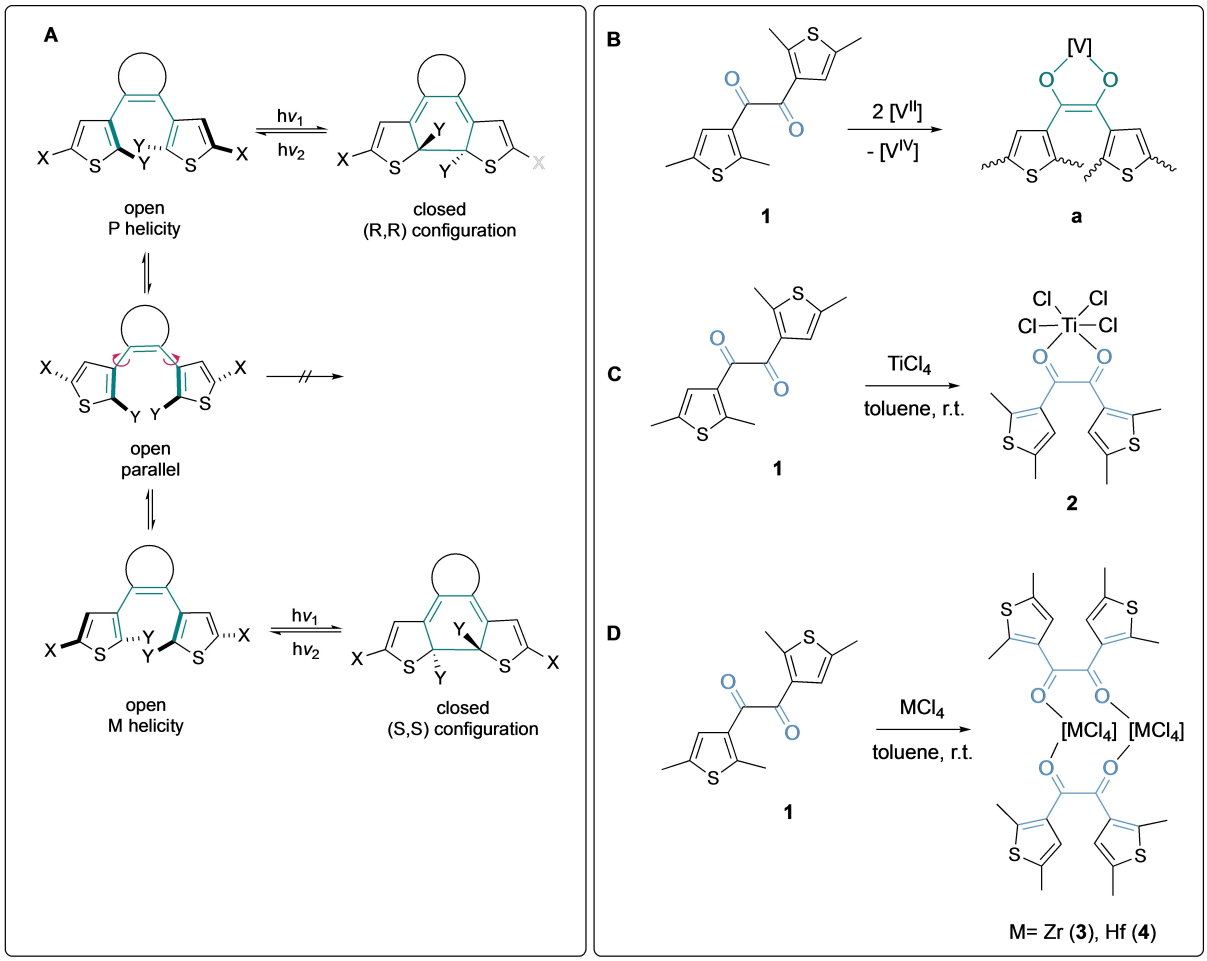

Scheme 1. A Generalization of the rotameric structures in dithienylethene photochromic switches (DTE); B *in-situ* reduction of 1,2-diketone (1) by V(II) to form a $[VO_2C_2]$ en-diolato metallacycle;[18] C and D Synthesis of complex **2**–**4.**

can be referred to as atropisomers. Atropisomerism, derived from Greek '*atropos*'=not turning, describes the hampered interconversion of rotamers about single bonds[23] and was first observed and studied in biaryl derivatives.[25] Atropisomerism finds application in design of chiral ligand systems, being applied in e.g. asymmetric catalysis,[26–30] medicinal chemistry[31] or as an alternative source for the production of chiral drugs.[32] It can also play an important role in modulation of molecular machines, where conformational change about a single bond is crucial.[33] Atropisomerism is a possible feature of DTEs.[22,34]

We have recently reported on the novel DTE-based complexes encompassing a five-membered metallacycle including an chelating en-diolato motif, which coordinates a vanadium(IV) metal center in direct proximity of the hexa-trien system (Scheme 1, **B**). The obtained compounds showed interesting interconversion of distinct atropisomers upon irradiation with UV light and evidence was observed for dynamic reversible C–C bond formation within the ligand backbone, indicating a fast cyclization/ring-opening in solution.[18] The synthesis involved the *in-situ* reduction of the pre-ligand 1,2-bis(2,5-dimethylthiophen-3-yl)ethane-1,2-dione (**1**, *DTEthane*) to the corresponding en-diolato motif (1,2-bis(2,5-dimethylthiophen-3-yl)ethene-1,2-diolate) by an excess of the V(II) precursor. Against this background, we now report on the direct complexation of **1** to MCl_4 metal precursors of the titanium triad (M=Ti, Zr, Hf) as shown in Scheme 1 **C** and **D**..

Results and Discussion

A solution of **1** in toluene reacts instantaneously with the respective MCl_4 (M=Ti, Zr, Hf) precursors to furnish dark red to black precipitates, which could be recrystallized from DCM/*n*-hexane. The obtained crystals were also suitable for single crystal X-ray diffraction (scXRD) analysis, which gave rise to the molecular structures of complex $[Ti(\kappa^2\text{-}O,O\text{-DTEthane})Cl_4]$ (**2**), $[Zr(\mu^2,\eta^1,\eta^1\text{-}O,O'\text{-DTEthane})Cl_4]_2$ (**3**), and $[Hf(\mu^2,\eta^1,\eta^1\text{-}O,O'\text{-DTEthane})Cl_4]_2$ (**4**). Selected interatomic distances for **1-4** are summarized in Table 1. As the Ti(IV) metal precursor is fully oxidized an *in-situ* reduction of **1** as previously observed for V(II) precursors,[18] is precluded and **1** gives rise to a chelating 1,2-diketone ligand (k^2-*O*,*O*-DTEthane, **1**). This is reflected in the obtained structure of **2** by a rather typically C=O interatomic distance of 1.247(2) Å and 1.251(2) Å, respectively only margin-

Research Article
doi.org/10.1002/ejic.202300276

Table 1. Selected bond lengths for diketone ligand **1** and complexes **2**–**4** in Å.

	1[i]	**2** (M=Ti)	**3** (M=Zr)	**4** (M=Hf)
C1–C7	1.467(2)	1.432(2)	1.414(4)	1.418(3)
C7–C8	1.540(2)	1.541(3)	1.527(4)	1.531(3)
C8–C9	1.467(2)	1.425(2)	1.428(4)	1.420(3)
C7–O1	1.224(2)	1.247(2)	1.245(4)	1.253(3)
C8–O2	1.224(2)	1.251(2)	1.244(4)	1.252(3)
O1–M1	–	2.137(1)	2.179(2)	2.171(2)
O2–M1	–	2.112(2)	2.192(2)	2.158(2)

[i]P. Pakulski, D. Pinkowicz.[35]

ally elongated with respect to the free ligand (1.224(2) Å in **1**)[35] and a C7–C8 interatomic distance of 1.541(3) Å, which is in good agreement for a typical C–C single bond. The coordinated carbonyl groups exhibit a O–C–C–O torsion angle of 19.2°. The Ti center resides in an octahedral coordination sphere built by four chlorido ligands and the chelating k^2-*O,O*-DTEthane ligand.

The thiophene rings in the coordinated ligand **1** reside in mutual *syn* alignment with respect to the C–H moiety and remain only slightly shifted from coplanarity with respect to the adjacent carbonyl group (torsion angles in **2**: O2–C8–C9–C10 = 17.9°; O1–C7–C1–C2 = 26.6°). This remarkable structural feature may imply that the π-conjugation in ligand **1** is effective and gives rise to coplanarity (which can be also observed in the structure of the free ligand)[35] resulting in one possible chiral axis along the C7–C8 bond (Figure 1, Scheme 2 **F**, **G**). Consequently, two enantiomers (*R* and *S*) exist for complex **2** (Scheme 2 **G**). In fact, compound **2** crystallizes as racemic mixture in the monoclinic space group $P2_1/n$ with a full molecule in the asymmetric unit.

In sharp contrast, the previously reported related en-diolato complexes[18] (Scheme 1, **a**) show strictly planar –V-(–O–C=C–O–) metallacycles with very small –O–C=C–O– torsions around 0.4°–4.5° and short C=C bonds with thiophene rings strongly deviating from coplanarity with respect to the metallacycle suggesting the presence of two possible C–C chiral axes along the 3-position of the thiophene rings and the endiolato backbone (Scheme 2, **E**). Similar structural features for five-membered metal chelated rings are reported by Sheng-Hua Liu, Zhong-Ning Chen and co-workers for related dithienyl-dithiolene chelated species **b**[19] and by Wolf and co-workers for copper complexes with DTE ligands carrying an 1,2-bisphosphane motif **c**.[20]

Complex **3** and **4** crystallize in the triclinic space group P-1 with half of the molecule in the asymmetric unit. In contrast to **2**, the molecular structures obtained for complexes **3** and **4**, formed between **1** and $ZrCl_4$ or $HfCl_4$, respectively, are dimeric: Two MCl_4 metal fragments are bridged by two {μ^2,η^1,η^1-*O,O′*-DTEthane} ligands furnishing a 10-membered metallacycle $(MO_2C_2)_2$. This structural composition may be preferred due to the larger ionic radii of the heavier congeners zirconium and hafnium (see also analysis based on DFT calculations below). The two DTEthane ligands bind with their respective μ^2,η^1,η^1-*O,O′* donors each metal center in mutual *cis*-position. Both diketone ligands in **3** and **4**, respectively, show O1–C7–C8–O2 torsions of almost 90° with the thiophene rings located almost orthogonal to each other and with inter plane angles (calculated as average planes through the five-membered thiophene rings) of 86° (**3**) and 84° (**4**), respectively. Similar to complex **2**, the molecular structures of **3** and **4** suggest that π-conjugation in ligand **1** results in coplanarity of the thiophene rings and the adjacent carbonyl group giving rise to only one possible chiral axis (C7–C8) as rotation about the C8–C9 and C1–C7 bonds may be hampered (Scheme 2, **F**). The two centrosymmetric molecular scXRD structures of **3** and **4** exhibit their two respective DTEthane ligands in *R* and *S* configuration and can therefore be identified as achiral *meso* isomers.

The ^{1}H NMR chemical shifts of complex **2** remained similar with respect to free ligand **1** except for the methyl group adjacent to the 2-position of the thiophene ring (see SI, CH_3 group label a), which displays a more significant shift from 2.70 ppm to 2.96 ppm upon coordination of **1** to the titanium

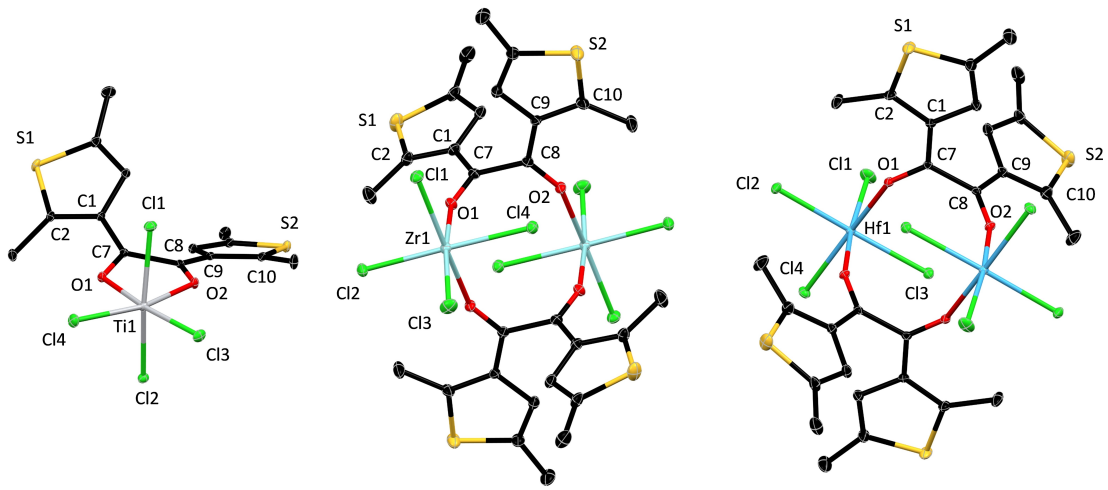

Figure 1. Mercury plots of the molecular structures of complex **2**–**4** derived from scXRD analysis. Thermal ellipsoids drawn at 30% probability. H-Atoms omitted for clarity.

Research Article
doi.org/10.1002/ejic.202300276

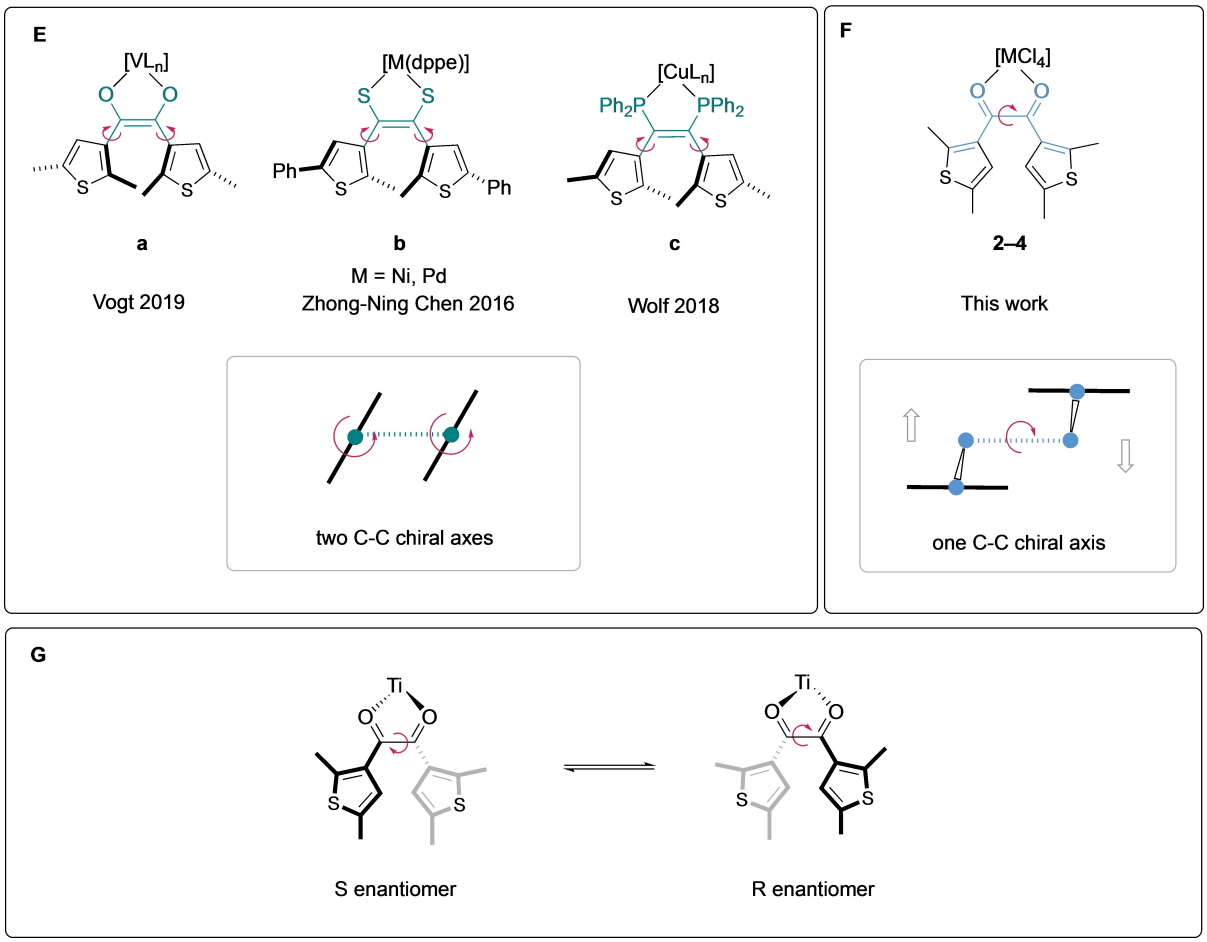

Scheme 2. Axial chirality features in complex **2**–**4** (F,G) and the previously reported examples **a**–**c** (E).

center. The resonances in the $^{13}C\{^1H\}$-NMR spectrum are marginally shifted with exception of the signals associated with the carbonyl-group (coordination shift of almost 3.2 ppm upfield), the quaternary C nucleus in 2-position of the thiophene ring (shift of 18.0 ppm downfield, see SI label b) and the C-atom of the methyl group adjacent to the 2-position of the thiophene ring, showing a shift from 16.1 ppm to 18.8 ppm upon coordination to the $TiCl_4$-fragment. Overall the $^{13}C\{^1H\}$-NMR chemical shifts suggest the conservation of the 1,2-ketone structural motif in **2**.

Complexes **3** and **4** are poorly soluble in dcm-d_2 and show rapid decomposition in coordinating solvents such as thf or acetonitrile. The ^1H NMR spectra of complex **3** and **4** are similar to **2**. However significant broadening is observed, which points toward solution dynamic processes. The $^{13}C\{^1H\}$ NMR spectra are substantially different: We observe seven resonances for **2** (half set) indicating a central molecular plane of symmetry.

In contrast, $^{13}C\{^1H\}$-NMR spectra of **3** and **4** reveal 28 resonances indicating significantly reduced symmetry with respect to **2**. Such an observation might be caused by partial dissociation[36] or a non-centrosymmetric arrangement of the diketone ligand in solution.

DFT Calculations

Quantum chemical investigations based on density functional theory (DFT) were performed on B97D3[38]/def2-TZVP[37,39] level of theory to gain further insights on the relative stability of monomers and dimers as well as the potential racemization pathways within this series. In line with the experimental findings we found that the monomeric complex **2** is 2.8 kcal·mol^{-1} more stable in Gibbs energy than the corresponding dimer, whereas for zirconium (**3**, ΔG =-3.9 kcal·mol^{-1}) and hafnium (**4**, ΔG =-5.9 kcal·mol^{-1}) the dimer was calculated to be more stable in solution (Table 2). A closer look at the optimized geometries of **2**–**4** reveal that each carbonyl group remains conjugated to the attached thiophene substituent and therewith in the same plane with respect to the substituent. This holds true for the monomeric, as well as the dimeric species. For the monomeric species the increased distance of the ligating atoms from titanium to hafnium results in an increased twist angle ($\angle_{OCCO}$ 26.0°… 36.4°), which in case of zirconium and hafnium leads to an increased stability of the dimer ($\angle_{OCCO}$ 98.8°/98.0°).

With view on the monomeric species we investigated the pathway of isomerization for the group four metals and found

Research Article
doi.org/10.1002/ejic.202300276

Table 2. Relative Gibbs energies based on DFT calculation (G16, B97D3/def2-TZVP).

metal	ΔG(dimer – 2·monomers)* kcal·mol^{-1}	ΔG_{rel}(R-isomer)/kcal·mol^{-1}	ΔG_{rel}(TS)/kcal·mol^{-1}	ΔG_{rel}(S-isomer)/kcal·mol^{-1}
Ti	+2.8	0	+13.1	+0.9
Zr	−3.9	0	+12.3	-0.8
Hf	−5.9	0	+12.2	+0.7

*SMD solvation model for CH_2Cl_2 was used.

that the difference in Gibbs energy between the *S*- and the *R*-isomer (Scheme 2 **G**) is with 0.7 to 0.9 kcal·mol^{-1} within the typical error of DFT calculations (Figure 2). It becomes evident that the barrier for racemization is the highest for titanium ($\triangle G_{rel}$(TS) = 13.1 kcal·mol^{-1}), followed by zirconium ($\triangle G_{rel}$(TS) = 12.3 kcal·mol^{-1}) and hafnium ($\triangle G_{rel}$(TS) = 12.2 kcal·mol^{-1}). In all complexes (**2**–**4**) the transition states are characterized by an imaginary vibration, involving contrary rotations of both thiophene rings (about two C–C rotational axes (C1–C7; C8–C9)) and a loss of conjugation rather than a direct rotation around the axis formed by the two carbonyl carbon atoms (C7–C8).

Conclusions

We report on the complexation of the 1,2-diketone ligand 1,2-bis(2,5-dimethylthiophen-3-yl)ethane-1,2-dione (**1**, *DTEthane*) to MCl_4 metal precursors of group four (M=Ti, Zr, Hf). While complex **2** with a Ti center shows a monomeric structure, related complexes with a Zr (**3**) or Hf (**4**) center gave rise to dimeric scaffolds with bridging {μ^2,η^1,η^1-*O*,*O*′-DTEthane} (**1**). DFT calculations (G16, B97D3/def2-TZVP, SMD solvation model = CH_2Cl_2) suggest a general trend of dimer formation in order of Ti < Zr < Hf and reveal the carbonyl groups residing in conjugation with their adjacent thiophene substituent, that is, the carbonyl unit as well as the adjacent thiophene ring are coplanar in monomer **2** as well as in the dimers **3** and **4**. Hence the rotation about the two C–C axes (C1–C7; C8–C9) is hampered. We have identified this structural feature as decisive for the nature and number of the chiral axes with respect to the closely related complexes with a five-membered metallacycle carrying the en-diolato ligand (1,2-bis(2,5-dimethylthiophen-3-yl)ethene-1,2-diolate, Scheme 1, **B**, **a**),[18] which encompass thiophene rings that are not coplanar to their neighboring five-membered metallacycle. While the latter results in two C–C chiral axes leading to chiral helicity (Scheme 2, **E**), the former gives rise to only one chiral axis (C7–C8) thus bringing forth axial chirality as, for instance, observed for classical biaryl compounds (Scheme 2, **F**). The barriers for racemization of complex **2** and the hypothetical monomers [Zr(**1**)Cl_4] and [Hf(**1**)Cl_4] follow the trend Ti > Zr > Hf. Noteworthy, the identified transition states are characterized by an imaginary vibration, involving counter-rotations of both thiophene rings.

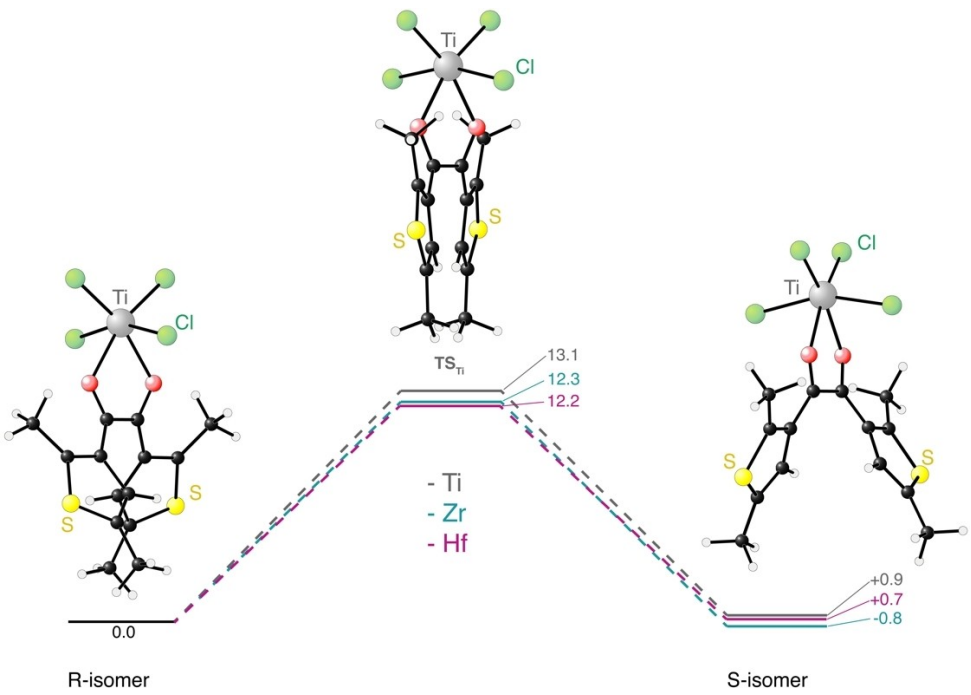

Figure 2. Calculated pathway for the racemization of **2** and the hypothetical monomers [Zr(**1**)Cl_4] and [Hf(**1**)Cl_4]. Gibbs energies based on DFT calculation (G16, B97D3/def2-TZVP) in kcal/mol^{-1}.

Research Article
doi.org/10.1002/ejic.202300276

That is, the interconversion of the *R*- and *S*-isomer proceeds *via* loss of conjugation due to the counter-rotation about the C1–C7 and C8–C9 axis rather than *via* involvement of the rotation about the C7–C8 single bond.

In summary one may state that in contrast to the en-diolato ligand motif **a**, the direct coordination of **1** to a fully oxidized group four $M^{(IV)}$ metal fragment does not furnish a hexa-trien system, which is a prerequisite for a photo-switchable system via a pericyclic ring-opening/ring-closure reaction scheme.[40] However, the herein reported coordination motif in complex **2**–**4** gives rise to remarkable structural features with relevance to the characteristics of the chiral axes.

Experimental Section

Metal tetrachlorides were obtained commercially (Sigma Aldrich, Alfa Aesar) and used as received. Dry solvents were collected from a SPS800 mBraun solvent system. Diketone **1** was prepared following a previously reported procedure.[18] *NMR*: ^{1}H-, ^{13}C-, and 2D NMR spectra were recorded at room temperature on a Bruker Avance Neo 600 MHz and a Bruker Avance 360 MHz spectrometer. Chemical shifts (δ) are reported downfield from tetramethylsilane in parts per million (ppm). Residual solvent signals (5.32 ppm for ^{1}H, 53.84 ppm for ^{13}C in CD_2Cl_2) were used as references. ^{1}H NMR coupling constants (J) are reported in Hertz (Hz), multiplicity is appointed as follows: s (singlet), m (multiplet). Assignments of ^{1}H and ^{13}C resonance signals were based on COSY, HSQC and HMBC spectra. *UV/VIS Spectroscopy*: Experiments were carried out at 298 K on a Varian Cary 50 UV/VIS-spectrophotometer. Cuvettes: 10 mm, synthetic quartz (QS) with Teflon cap. Samples were prepared under an inert atmosphere of argon.

Complex 2: (80 mg, 0.29 mmol, 1.1 eq.) was dissolved in 5 mL toluene and treated with $TiCl_4$ (29 µL, ϱ = 1.73 g/cm^3, 0.26 mmol, 1.0 eq.). Instantly a dark red precipitate occurred. The suspension was stirred at rt for 2 h before removal of the solvent under reduced pressure and washing the crude product with small portions of *n*-hexane led to **2** as dark red to black solid. Crystals suitable for X-ray crystallography were obtained *via* slow diffusion of *n*-hexane into a saturated solution of **2** in DCM. **Yield**: 110 mg (0.23 mmol, 89%); **Mp:** > 200 °C dec.; **^{1}H NMR**: (360 MHz, CD_2Cl_2): δ 6.90 (s, 2H, c), 2.96 (s, 6H, a), 2.42 (s, 6H, b) ppm; **^{13}C NMR**: (90 MHz, CD_2Cl_2): δ 186.5 (g), 169.9 (b), 138.7 (c), 130.6 (a), 127.9 (d), 18.8 (e), 15.2 (f) ppm; **UV/Vis** (CH_2Cl_2): λ_{max} = 270 nm; $\lambda_{shoulder}$ = 314 nm.–

Complex 3: (80 mg, 0.29 mmol, 1.1 eq.) was dissolved in 5 mL toluene and treated with $ZrCl_4$ (60 mg, 0.26 mmol, 1.0 eq.). Instantly a dark red precipitate occurred. The suspension was stirred at rt for 2 h before removal of the solvent under reduced pressure and washing the crude product with small portions of *n*-hexane led to **3** as orange to brown solid. Crystals suitable for X-ray crystallography were obtained *via* slow diffusion of *n*-hexane into a saturated solution of **3** in DCM. **Yield**: 120 mg (0.12 mmol, 90%), **Mp**: > 75 °C dec.; **^{1}H NMR**: (600 MHz, CD_2Cl_2): δ 7.00–6.90 (m, 4H, thienyl), 3.02–2.84 (m, 12H, thienyl-Me), 2.47–2.38 (m, 12H, thienyl-Me) ppm; **^{13}C NMR**: (150 MHz, CD_2Cl_2): δ 188.1, 179.4, 171.2, 167.5, 155.8, 148.2, 138.7, 138.1, 132.8, 131.2, 129.4, 128.0, 124.7, 121.8, 121.3, 120.1, 39.1, 38.6, 32.0, 30.1, 26.9, 26.0, 23.1, 19.8, 16.6, 15.2, 14.3, 13.9 ppm; **UV/Vis** (CH_2Cl_2): λ_{max} = 273, 459 nm; $\lambda_{shoulder}$ = 318 nm.

Complex 4: **1** (80 mg, 0.29 mmol, 1.1 eq.) was dissolved in 5 mL toluene and treated with $HfCl_4$ (80 mg, 0.26 mmol, 1.0 eq.). Instantly a dark red precipitate occurred. The suspension was stirred at rt for 2 h before removal of the solvent under reduced pressure and washing the crude product with small portions of *n*-hexane led to **4** as orange to brown solid. Crystals suitable for X-ray crystallography were obtained *via* slow diffusion of *n*-hexane into a saturated solution of **4** in DCM. **Yield**: 141 mg (0.12 mmol, 90%), **Mp:** > 80 °C dec.; **^{1}H NMR**: (600 MHz, CD_2Cl_2): δ 7.00–6.90 (m, 4H, thienyl), 3.11–2.90 (m, 12H, thienyl-Me), 2.48–2.39 (m, 12H, thienyl-Me) ppm; **^{13}C NMR**: (150 MHz, CD_2Cl_2): δ 187.5, 174.5, 172.3, 168.3, 139.3, 138.2, 134.8, 132.7, 131.5, 131.2, 129.5, 128.9, 128.3, 120.0, 39.3, 32.3, 32.0, 30.1, 29.6, 26.0, 23.1, 20.7, 20.0, 19.6, 16.6, 15.2, 14.3, 13.9 ppm; **UV/Vis** (CH_2Cl_2): λ_{max} = 273, 518 nm; $\lambda_{shoulder}$ = 318 nm.

CCDC Deposition Numbers 2256655(for **2**), 2256654(for **3**), 2256653(for **4**) contain the supplementary crystallographic data for this paper. These data are provided free of charge by the joint Cambridge Crystallographic Data Centre and Fachinformationszentrum Karlsruhe Access Structures service.

Supporting Information

The Supporting Information is available free of charge.

DFT-optimized geometries (XYZ).

NMR spectra, UV/Vis spectra and Cyclic voltammograms (PDF).

Acknowledgements

M.V. wants to acknowledge the generous financial support by the Fonds der Chemischen Industrie (FCI) and the Central Research and Development Fund (CRDF) of the University of Bremen. Open Access funding enabled and organized by Projekt DEAL.

Conflict of Interests

The authors declare no conflict of interest.

Data Availability Statement

The data that support the findings of this study are available in the supplementary material of this article.

Keywords: atropisomerism · chiral axes · carbonyl ligands · dithienylethene · titanium

[1] M. Irie, *Chem. Rev.* **2000**, *100*, 1685–1716.
[2] K. Szaciłowski, *Chem. Rev.* **2008**, *108*, 3481–3548.
[3] S. Pu, D. Jiang, W. Liu, G. Liu, S. Cui, *J. Mater. Chem.* **2012**, *22*, 3517–3526.
[4] G. Jiang, S. Wang, W. Yuan, L. Jiang, Y. Song, H. Tian, D. Zhu, *Chem. Mater.* **2006**, *18*, 235–237.
[5] J. Andréasson, S. D. Straight, T. A. Moore, A. L. Moore, D. Gust, *J. Am. Chem. Soc.* **2008**, *130*, 11122–11128.
[6] H. Tian, *Angew. Chem. Int. Ed.* **2010**, *49*, 4710–4712.
[7] S.-Z. Pu, Q. Sun, C.-B. Fan, R.-J. Wang, G. Liu, *J. Mater. Chem. C.* **2016**, *4*, 3075–3093.
[8] H.-H. Liu, Y. Chen, *Dyes Pigm.* **2011**, *89*, 212–216.
[9] C. P. Harvey, J. D. Tovar, *Polym. Chem.* **2011**, *2*, 2699–2706.
[10] S. Cui, G. Liu, S. Pu, B. Chen, *Dyes Pigm.* **2013**, *99*, 950–956.

[11] D. Frath, S. Yokoyama, T. Hirose, K. Matsuda, *J. Photochem. Photobiol. C* **2018**, *34*, 29–40.
[12] T. Hirose, K. Matsuda, *Org. Biomol. Chem.* **2013**, *11*, 873–880.
[13] C. Xiao, W.-Y. Zhao, D.-Y. Zhou, Y. Huang, Y. Tao, W.-H. Wu, C. Yang, *Chin. Chem. Lett.* **2015**, *26*, 817–824.
[14] M. Choudhari, J. Xu, A. I. McKay, C. Guerrin, C. Forsyth, H. Z. Ma, L. Goerigk, R. A. J. O'Hair, A. Bonnefont, L. Ruhlmann, S. Aloise, C. Ritchie, *Chem. Sci.* **2022**, *13*, 13732–13740.
[15] S. Kobatake, S. Takami, H. Muto, T. Ishikawa, M. Irie, *Nature* **2007**, *446*, 778–781.
[16] K. Uchida, S. Sukata, Y. Matsuzawa, M. Akazawa, J. J. de Jong, N. Katsonis, Y. Kojima, S. Nakamura, J. Areephong, A. Meetsma, B. L. Feringa, *Chem. Commun.* **2008**, 326–328.
[17] B. M. Neilson, V. M. Lynch, C. W. Bielawski, *Angew. Chem. Int. Ed.* **2011**, *50*, 10322–10326.
[18] D. Schlüter, F. Kleemiss, M. Fugel, E. Lork, K. Sugimoto, S. Grabowsky, J. R. Harmer, M. Vogt, *Chem. Eur. J.* **2020**, *26*, 1335–1343.
[19] J. Wang, L. X. Shi, J. Y. Wang, J. X. Chen, S. H. Liu, Z. N. Chen, *Dalton Trans.* **2017**, *46*, 2023–2029.
[20] Z. Xu, Y. Cao, B. O. Patrick, M. O. Wolf, *Chem. Eur. J.* **2018**, *24*, 10315–10319.
[21] B. L. Feringa, W. R. Browne, *Molecular Switches*, Wiley-VCH, Weinheim, **2011**.
[22] T. J. Wigglesworth, D. Sud, T. B. Norsten, V. S. Lekhi, N. R. Branda, *J. Am. Chem. Soc.* **2005**, *127*, 7272–7273.
[23] J. E. Smyth, N. M. Butler, P. A. Keller, *Nat. Prod. Rep.* **2015**, *32*, 1562–1583.
[24] M. Ōki, *Top. Stereochem.* **1983**, *14*, 1–81.
[25] G. H. Christie, J. Kenner, *J. Chem. Soc. Trans.* **1922**, *121*, 614–620.
[26] A. Miyashita, A. Yasuda, H. Takaya, K. Toriumi, T. Ito, T. Souchi, R. Noyori, *J. Am. Chem. Soc.* **1980**, *102*, 7932–7934.
[27] L. Pu, *Chem. Rev.* **1998**, *98*, 2405–2494.
[28] R. Noyori, *Angew. Chem. Int. Ed.* **2002**, *41*, 2008–2022.
[29] K. Mikami, M. Yamanaka, *Chem. Rev.* **2003**, *103*, 3369–3400.
[30] E. Kumarasamy, R. Raghunathan, M. P. Sibi, J. Sivaguru, *Chem. Rev.* **2015**, *115*, 11239–11300.
[31] P. W. Glunz, *Bioorg. Med. Chem. Lett.* **2018**, *28*, 53–60.
[32] J. Clayden, W. J. Moran, P. J. Edwards, S. R. LaPlante, *Angew. Chem. Int. Ed.* **2009**, *48*, 6398–6401.
[33] S. Erbas-Cakmak, D. A. Leigh, C. T. McTernan, A. L. Nussbaumer, *Chem. Rev.* **2015**, *115*, 10081–10206.
[34] G. W. Gribble, J. A. Joule, *Progress in Heterocyclic Chemistry* Elsevier, UK, **2009**, Vol. 30.
[35] P. Pakulski, D. Pinkowicz, *CSD Private Communication CCDC1895209* **2019**, 1–3.
[36] Note that we have observed facile dissociation of **1** in the presence of coordinating solvents such as thf. For NMR spectral details see Figure S9.
[37] F. Weigend, R. Ahlrichs, *Phys. Chem. Chem. Phys.* **2005**, *7*, 3297–3305.
[38] S. Grimme, S. Ehrlich, L. Goerigk, *J. Comput. Chem.* **2011**, *32*, 1456–1465.
[39] F. Weigend, *Phys. Chem. Chem. Phys.* **2006**, *8*, 1057–1065.
[40] Note that we also tried to react complexes **2–4** with potassium metal or KC_8 aiming for the two-electron-reduction of the ligand, which could allow for the formation of a hexa-trien motif in **1**. However, our attempts did not result in defined reaction products. A cyclic voltammetry study concerning this matter is included in the SI (Table S3, Figure S12).

Manuscript received: May 11, 2023
Revised manuscript received: May 22, 2023
Accepted manuscript online: May 24, 2023